

Title Page

USGS award number G11AP20050

Paul W. Jewell

**Rediscovering the Discovery Outcrop:
The Promises and Pitfalls of Digital Elevation Models
in Mineral Exploration**

Research supported by the U.S. Geological Survey (USGS), Department of the Interior, under USGS award number G11AP20050. The views and conclusions contained in this document are those of the authors and should not be interpreted as necessarily representing the official policies, either expressed or implied, of the U.S. Government.

Rediscovering the Discovery Outcrop:
The Promises and Pitfalls of Digital Elevation Models in Mineral Exploration

Paul W. Jewell
J. Anna Farnsworth
Theresa Zajac

Department of Geology and Geophysics
University of Utah
Salt Lake City, Utah 84112

ABSTRACT

An increasing number of mineral discoveries rely on remote sensing methods such as airborne geophysics and hyperspectral imaging. The relatively new technology of LiDAR, whereby surface outcrop patterns suggestive of economic mineralization can be identified, has the potential to join other remote sensing techniques employed by the exploration geologist. Successful application of LiDAR relies on rigorous, high-quality data collected under strict QA/QC standards and is most useful for delineating linear features such as faults or resistant lithologies such as silicification. If used judiciously, LiDAR can join the toolbox of the modern exploration geologist working in tropical and boreal forest areas that contain many of the most prospective terrains left on Earth.

INTRODUCTION

Until the 20th century, the discovery of new ore deposits relied on careful field work by professionals or the serendipitous realization of prospectors that a particular rock outcrop possessed valuable minerals. In mid- and high-latitude terrains, rock

outcroppings are often readily visible, meaning ore deposits close to the Earth's surface in these areas had largely been discovered by the close of the past century. The latter part of the 20th century saw increased reliance on geophysical methods and deep drilling to find ore deposits in both sparsely vegetated terrains of mid- and high-latitudes as well as expanding to unexplored frontiers in low latitudes.

In the late 20th and early 21st centuries, two factors shifted much exploration emphasis to tropical and boreal forest terrains. The first has been favorable political and economic liberalization and a drift away from state-directed enterprises in Asia, Africa, and South America (e.g., Tilton, 1988). Furthermore, the boreal terrains of Canada, Alaska, and Europe have become appealing for exploration as existing mineral districts of these countries played out or come under more stringent environmental overview.

While ground and airborne geophysics will continue to be a premier tool for exploration in boreal and tropical terrains, knowledge of surface geology as well as knowing where rock outcrops might be or whether they even exist in these areas will be critical for successful exploration efforts. To that end, the relatively new technology of LiDAR (for Light Detection and Ranging) with its ability to produce cm-scale terrain elevation data may become an important remote sensing tool in mineral exploration.

The underlying premise of using LiDAR in mineral exploration is that specific rock types and their associated alteration produce recognizable topographic patterns that are resolvable with standard LiDAR techniques. For instance, the silicification associated with a variety of porphyry and vein deposits is more resistant to weathering than surrounding country rock (Lovering, 1972; Hedenquist et al., 2000) producing a modest topographic high that may be visible with standard GIS software. Likewise,

argillic alteration, with easily weatherable clays could produce a recessive topographic signature.

This article reviews the basics of LiDAR technology and explores some of the utility and possible drawbacks of applying this technology to mineral exploration in the 21st century. Three areas with widely varying vegetation cover and LiDAR quality are examined for surficial and geologic features associated with hydrothermal ore deposits. The possibility of incorporating LiDAR with other airborne geophysical methods and becoming effective in exploring in areas considered difficult for traditional exploration methodologies is then considered

LIDAR BACKGROUND AND APPLICATIONS

As computing power has grown, digital elevation models (DEMs) have progressively increased in resolution, availability, and utility (Fig. 1) and gradually become a formidable tool for unraveling a variety of features on the surface of the Earth. Early DEMs relied on digitizing existing topographic maps or applying photogrammetric techniques to stereo aerial photography (e.g., Schenk, 1999). Subsequently, radar became a source for computing the distance from satellite or airborne platforms to the Earth's surface (e.g., Smith, 2002). However, neither photogrammetric nor radar methodologies effectively penetrate extensive vegetative cover and thus are of limited use for resolving very-fine scale features at the Earth's surface that are typically of interest to economic geologists who rely on very subtle topographic expression of ore deposit features in their work.

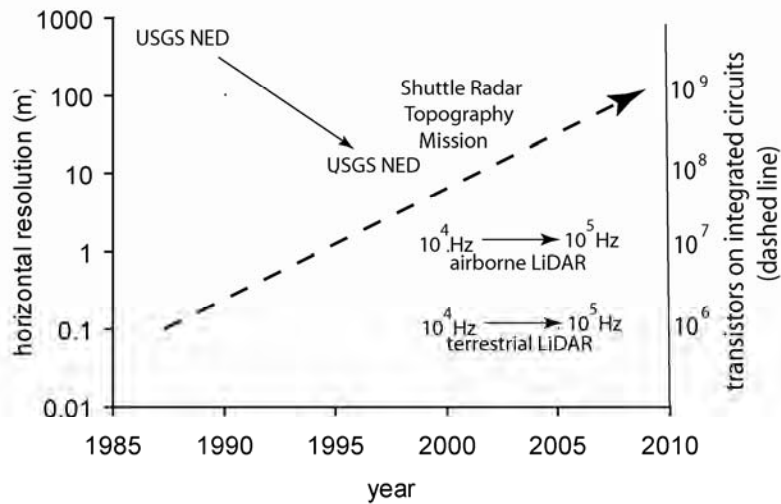


Figure 1. Timeline of technological developments in digital imaging of land surfaces. NED = National Elevation Data. The dashed line represents the right-hand horizontal axis, commonly referred to Moore's Law whereby available computing power doubles every three years.

In recent years LiDAR has been effectively applied to earth science as well as fields as diverse as art history and transportation engineering. Using a laser source, LiDAR is capable of producing remarkably fine-scale topographic maps and 3-dimensional images and can detect subtle surface features on a wide variety of scales. The method relies on sending and receiving coherent laser pulses (current technology at the rate of $\sim 10^5$ Hz) to the object being surveyed. LiDAR instruments can be mounted on airborne or ground-based (terrestrial) platforms.

Careful and sophisticated data acquisition and post-processing are necessary to achieve reliable and reproducible data. Airborne LiDAR must rely on kinematic aircraft GPS and static ground GPS to correctly georeference the data obtained from a moving aircraft high above the ground. Flight lines overlap such that redundant coverage is obtained between flight lines. Terrestrial LiDAR typically requires multiple scans from different perspectives in order to capture the 3-dimensional character of the scanned

object and, while georeferencing is not as difficult as for airborne data, stitching the multiple scans together can be a challenge.

All LiDAR instruments produce “point clouds”: individual x-y-z coordinate that may possess additional features such as relative intensity. A variety of methods are used to transform the irregularly spaced point cloud into the evenly spaced raster files necessary for modern rapid computer analysis. The resulting spatial resolution is a function of the number of returns per area: for airborne LiDAR, horizontal postings are generally 1-2 m while vertical resolution is on the order of a few centimeters. Terrestrial LiDAR resolution depends on the distance between the scanner and the target but can easily be at the mm scale.

Because the wavelength of the LiDAR source is small ($\sim 1 \mu\text{m}$), one of the crowning achievements of this technology is its ability to “see through” vegetation and forest canopies based on the last return of the laser pulses. In effect, post-processing of LiDAR data filters out returns from tree and vegetative cover to reveal important features of the underlying land surface. As a result, unknown or poorly characterized fault scarps and landslides have been discovered and mapped in heavily vegetated areas such as Puget Sound (e.g., Haaugerud, et al., 2003). LiDAR has gradually been employed in such fundamental activities as bedrock geologic mapping, principally involving delineating geologic structures (e.g., Pavlis and Bruhn, 2011) although more esoteric applications such as combining with hyperspectral investigations of geothermal areas (e.g., Silver et al., 2011) have appeared. Fine-scale outcrop mapping by terrestrial LiDAR has been effective in advancing the fields of both sedimentary and structural geology (Bellian et al., 2005; Jones et al., 2009).

Individual LiDAR pulses are generally recorded as a series of returns from the various surfaces encountered by the individual pulse. Thus, for airborne LiDAR, the first return is useful for documenting forest canopy heights in biological surveys. Geologists in turn are typically most interested in the last return of the pulse since this represents the ground surface where geologic features become manifest.

APPLICATION TO MINERALIZED AREAS

Examples of LiDAR coverage from three historic mining districts provide a contrast to show the possibilities and possible pitfalls of using this technology to understand alteration and mineralization in a variety of geologic settings. From early 2011 through 2012, the authors visited and mapped a variety of mining districts in Utah and Oregon for which existing LiDAR data were publically available. The three settings presented here represent a variety of geologic features, vegetation cover, and LiDAR data quality (Fig. 2) (Table 1) and are meant to illustrate some of the problems as well as the possibilities associated with this technology. A preliminary version of these results was presented at the December, 2011 national meeting of the Northwest Mining Association in Reno, Nevada.

Alta District, Utah

The Alta mining district (also known as the Little Cottonwood-American Fork district) in north-central Utah first became active in the 1860s and was productive until the period immediately following World War II. The district has largely produced from contact aureoles and fissures related to moderate-sized, intermediate for felsic intrusions that yielded mostly base metals and silver (Boutwell, 1912). The Alta district was

imaged as part of a 2006-2007 airborne LiDAR survey of the central Wasatch Front underwritten by the U.S. Geological Survey and a variety of local government entities.

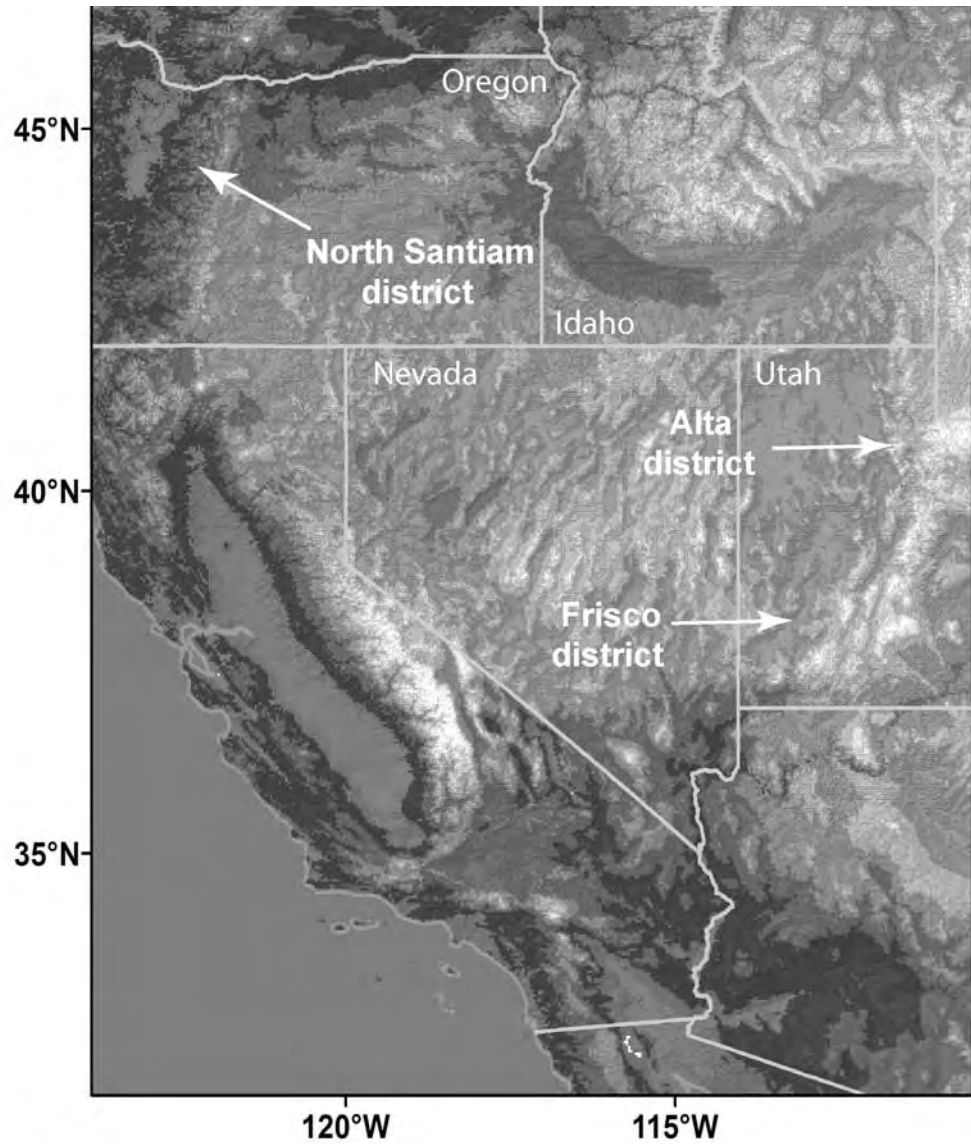


Figure 2. Location of the mineral districts (Alta, Utah; Frisco, Utah; and North Santiam, Oregon) that have been imaged with LiDAR and discussed in the paper.

Table 1. Characteristics of mining districts and LiDAR data sets employed in this study.

	Alta, Utah	Frisco, Utah	North Santiam, Oregon
Host rocks	Mesozoic sedimentary rocks; Tertiary intrusions	Lower Paleozoic carbonates; Tertiary intrusions	Tertiary intrusions
Alteration style	Mineralized fissures, skarns	Mineralized fissures, skarns	Mineralized veins
Ore deposit	Jupiter Mine (Ag, base metals)	Unnamed prospect (base metals)	Blue Jay mine (Au, base metals)
LiDAR availability	State of Utah Automated Geographic Reference Center	U.S. Department of Agriculture, Salt Lake City Office	Oregon LiDAR Consortium
LiDAR resolution	2-m horizontal	1-m horizontal	2-m horizontal

The area examined in specific detail is in Thaynes Canyon northeast of Alta and immediately west of the Park City mining district (Fig. 3). The eastward trending drainage is steep and heavily forested on the north-facing slopes. The little outcrop that exists is typically cloaked by vegetation or glacial till. The geology of the canyon consists of the Triassic Woodside Shale, a fine-grained dark-red shale; the Thaynes Formation, a limy sandstone; and the Ankarah Formation composed of sandstone, mudstone, and shale. The contact aureole is associated with the Clayton Peak Stock, a mid-Tertiary quartz monzodiorite (Bromfield 1989) that has been intruded by a series of intermediate dikes that trend NE-SW. In places, the porphyries exhibit propylitic alteration with epidote replacing feldspars and mafic minerals. The Jupiter Mine in the bottom of Thaynes Canyon produced silver and base metals from NE-trending fissures (Boutwell, 1912).

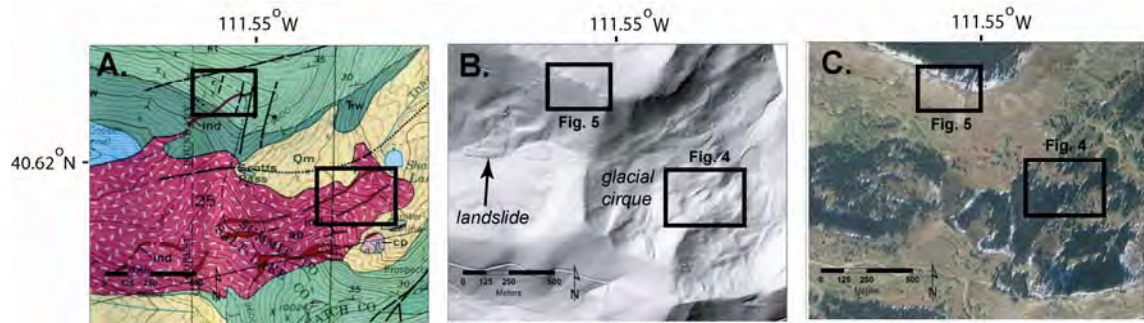


Figure 3. A. Geologic map of a portion of Brighton quadrangle in the Alta mining district of Utah (Baker et al., 1966). Qm = Quaternary morrain material, ind = intermediate dikes (Tertiary), ap = porphyry of the Clayton Peak stock (Tertiary), Trt = Thaynes formation (Triassic), Trw = Woodside Formation (Triassic). Boxes show areas of Figures 4 and 5. B. Hillshade of LiDAR-derived DEMs of the area in A. C. National Agricultural Imagery Program (NAIP) photograph of the area in A and B.

LiDAR shows a landslide feature not visible in aerial photography or documented on the geologic map of the area (Fig. 3). The valley area was glaciated in the Quaternary and is still largely covered by glacial deposits. Several lateral moraines appear to align with the intermediate dikes mapped by Baker et al. (1966) on the LiDAR image (Fig. 4). Field examination by the authors was not able to define a definitive northeast outcrop trend of the intermediate dikes in the field, although there is a suggestion of such a feature in the LiDAR (Fig. 4B). Neither the moraines nor the dikes are apparent in the aerial photograph (Fig 4A).

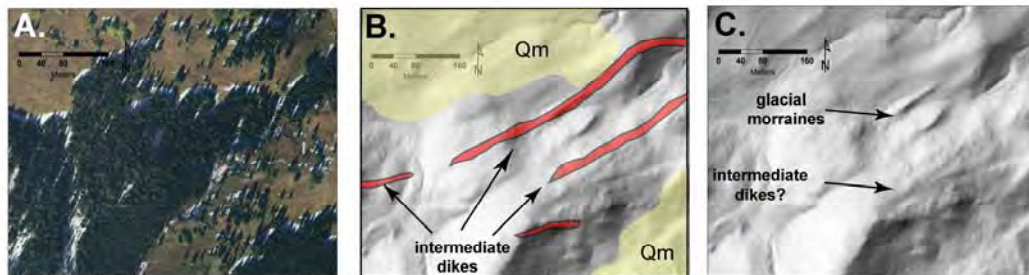


Figure 4. Detail of cirque area shown in Figure 3. A. NAIP digital photograph of the Shadow Lake area. B. Detailed hillshade of the Shadow Lake cirque area with overlain geologic features. C. Details of the features in the Shadow Lake cirque area.

On the ridge north of the canyon, the Thaynes and Woodside Formations are clearly offset by NNE-trending faults visible in both the aerial photo and LiDAR hillshade (Fig. 5). The bedding plane visible in the LiDAR provides an opportunity to compare bedding orientations collected in the field with those derived the freeware MICRODEM program (available through the U. S. Naval Academy). Three points picked by MICRODEM produces an orientation (N64°W, 35°NE) that compared favorably with orientations collected by the authors (N60°W, 30°NE) as well as those shown on the geologic map of Baker et al. (1966).

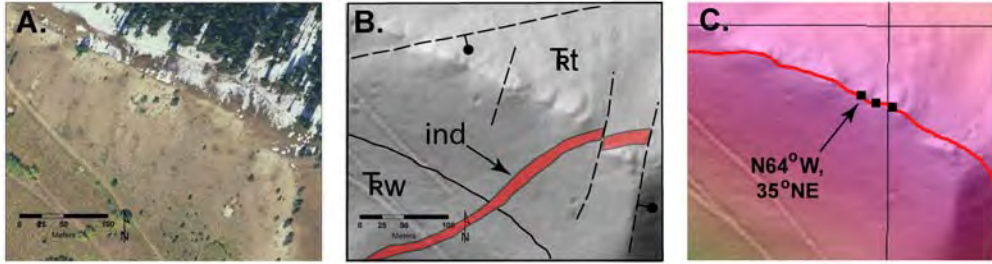


Figure 5. Detail of ridgeline geology shown in Figure 3. A. NAIP digital photograph of the ridge in the northern portion of the Shadow Lake area. B. Detailed hillshade of the Shadow Lake cirque area. C. Detailed geologic map of the Shadow Lake cirque area.

Frisco District, Utah

The Frisco mining district is located in the San Francisco Mountains ~40 km west of Milford, Utah (Fig. 2). Although the Horn Silver Mine in the eastern portion of the district was a large producer of silver and base metals in the late 19th and early 20th centuries (Butler, 1913, 1914), very little modern geologic research has been conducted on the district. Rocks are largely lower Paleozoic carbonates intruded and extensively altered by granodiorite of the Oligocene Cactus stock (Hintze et al., 1984). The majority of the mineralization consists of contact replacement and fissure deposits associated with the Cactus stock. Major ore deposits are found in both the intrusive rocks and as replacements of the surrounding carbonates with significant oxidation of the sulfides in the upper portions of the deposits (Butler, 1914).

The area examined in detail is immediately south of the Indian Queen mine on the west flank of the San Francisco Mountains. The main workings are in skarn of the Cambrian Big Horse Limestone where it was intruded by the Cactus stock. Limestone to the north has been extensively altered, recrystallized, and is locally ferruginous (Fig. 6). The area is covered by a very sparse juniper forest, thus permitting a comparison between features seen in the field, on aerial photography, and with DEMs.

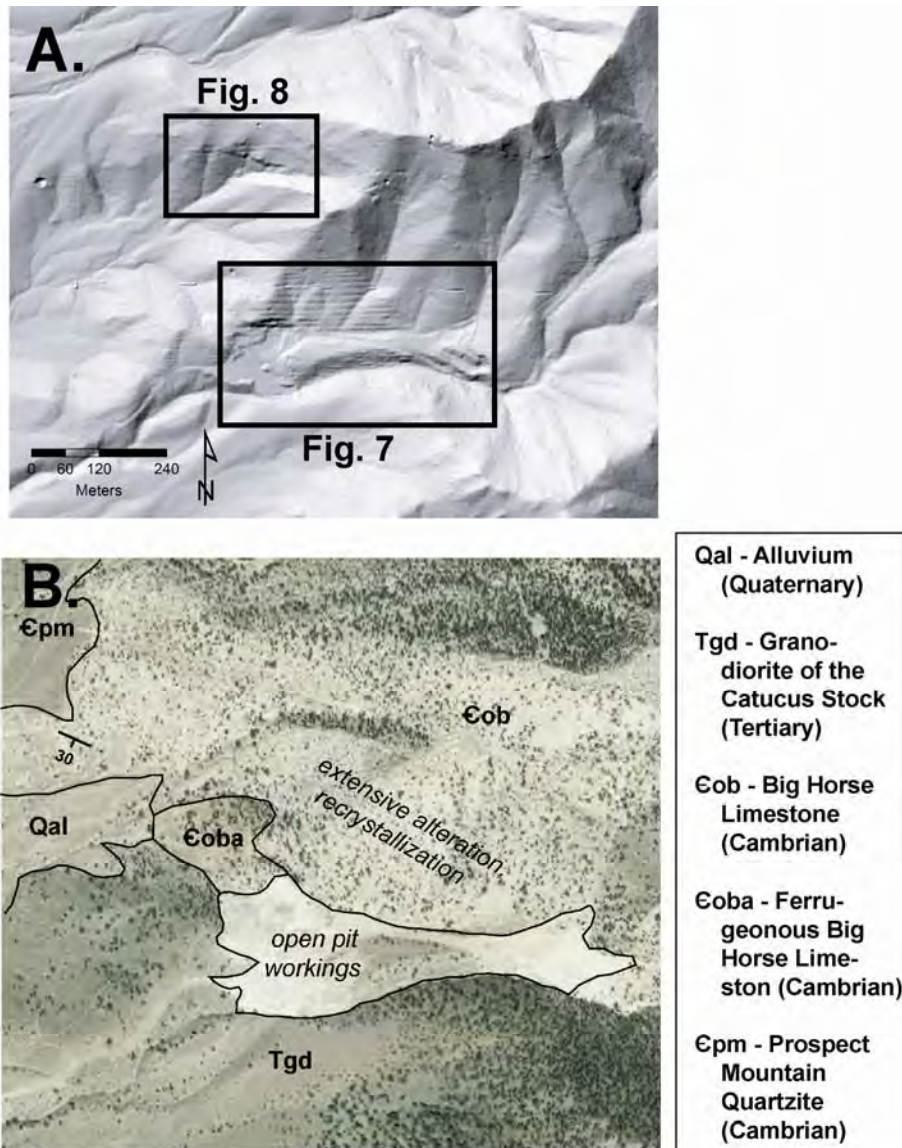


Figure 6. A. Hillshade of LiDAR-derived DEMs of the area south of the Indian Queen mine, Frisco mining district Utah. Square shows area of Figures 7 and 8. B. Generalized geologic map of the Indian Queen mine area (Jewell, unpublished).

LiDAR data near the Indian Queen mine are part of a larger survey acquired by a U.S. Department of Agriculture to study the hydrology of the Wah Wah Valley to the west (Meier, 2005). Only a small portion of the western edge of the Frisco district was covered by the survey. Problems associated with LiDAR coverage in this area are clearly

apparent in GIS-produced hillshades of the area (Fig. 6). Horizontal linears are obvious and appear to be present where two flight lines of the survey overlapped (Fig. 7). The stair-stepped topographic profile of the area (Fig. 7C) is suggestive of an offset in georeferencing between the two flight lines, although a post-processing error in the data cannot be discounted.

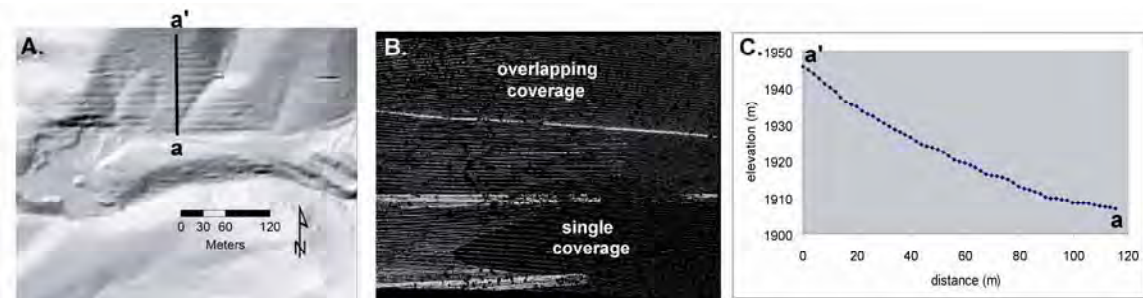


Figure 7. A. Hillshade of LiDAR DEMs of the Indian Queen mine area. B. Detail of Frisco mining district show misaligned LiDAR swaths. C. Cross section of DEM data from along line a-a'

In spite of the problems with the LiDAR data in this area, the utility of this technique is illustrated by a close examination of rocks north of the main Indian Queen workings. A rusty, WNW-trending zone of silicified limestone (jasperoid) is readily apparent in the field as well as the LiDAR hillshade, yet is virtually invisible on the aerial photo (Fig. 8). Were this mineralized feature located in an area of dense vegetation, the LiDAR would have been very useful in pinpointing an area for the exploration geologist to investigate and sample.

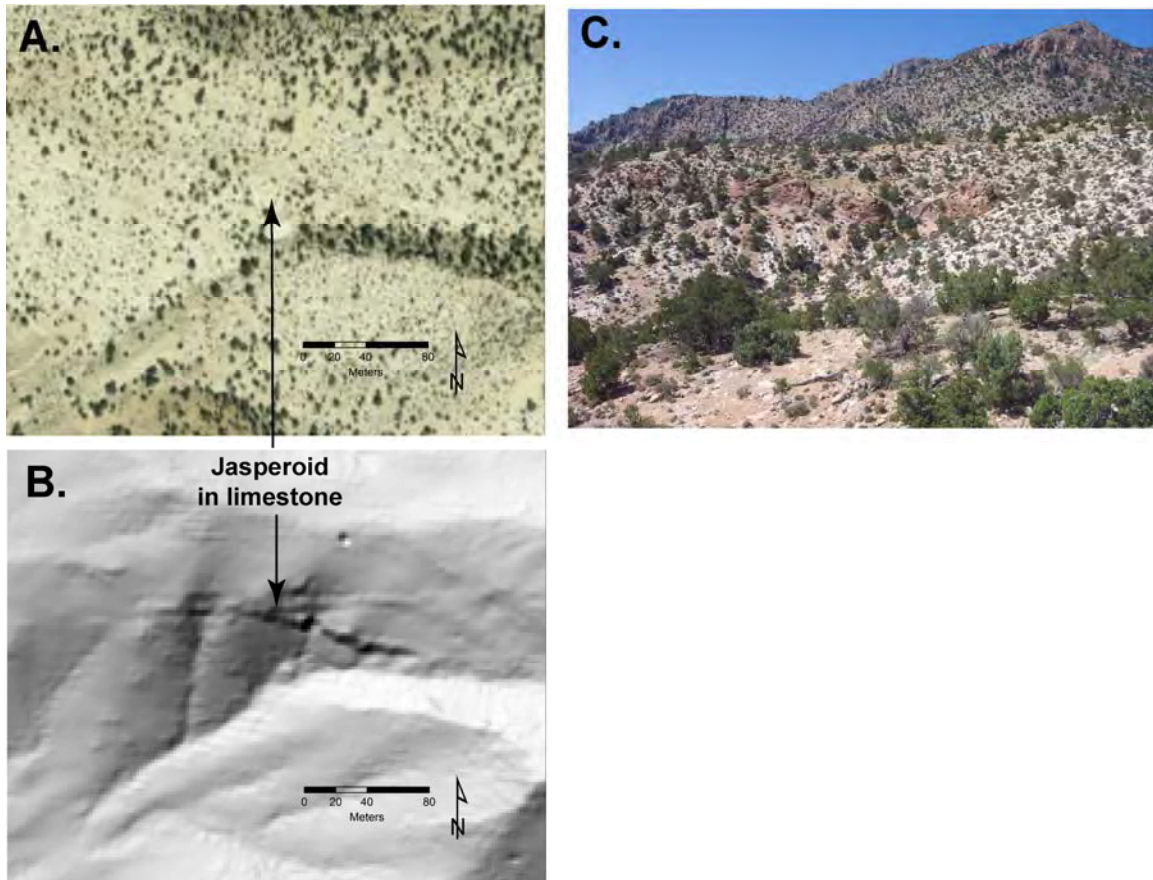


Figure 8. A. NAIP photograph of area immediately south of the Indian mine. B. Hillshade of LiDAR-derived DEMs of the area in A. C. Field photography of WNW-trending silicified zone (jasperoid) in limestone.

North Santiam District, Oregon

The North Santiam district is located in the central Cascade Mountains of Oregon (Fig. 2), an area dominated by Cenozoic volcanic rocks of varying but generally intermediate composition. The dominant host lithology of the North Santiam district is Oligocene andesite. Labradorite andesite is found in localized areas. Intrusive dikes in the district are comprised of dacite porphyry that typically trend to the northwest. The primary mineralization of the small vein deposits is chalcopyrite, sphalerite, pyrite, galena, and gold. The veins consist of (1) complex sulfide veins with sphalerite as the primary sulfide and variable amounts of pyrite, galena, and chalcopyrite; (2) pyrite veins

with pyrite as the primary sulfide and variable amounts of chalcopyrite, sphalerite, and galena; (3) bimetallic veins which are a transition between complex sulfide veins and pyrite veins; and (4) chalcopyrite veins with chalcopyrite as the primary sulfide and variable amounts of pyrite, sphalerite, and galena. The primary gauge minerals in the district are quartz and calcite. The alteration within the district is sericitic and propylitic alteration with localized argillic alteration. Epidote, chlorite, sericite, calcite, quartz, and clay minerals around veins and on fractures are evidence of these alterations (Callaghan and Buddington, 1938).

The LiDAR analysis focused on two areas of prospects and underground workings (Ruth and Blue Jay mines) near the headwaters of the Little North Santiam River. The LiDAR data were obtained through the Oregon LiDAR Consortium's Willamette Valley project. LiDAR data are posted at 1-m horizontal spacings and available at nominal cost through the Oregon Department of Geology and Mineral Industries or in some cases is free through the OpenTopography website.

The North Santiam area is characterized by extremely rugged topography with dense conifer forest and undercover vegetation (Fig. 9A). In this setting, considerable information regarding the pros and cons of LiDAR can be discerned. The detail seen in the DEMs is directly related to the density of laser shots that reach the ground (Fig. 9B, C). While access roads to the mined area and drainages are visible on aerial photographs (Fig. 10A), LiDAR hillshades show very distinctly the location of outcrops and adits (Fig. 10B, C). Where laser shot density is very sparse, holes in the DEMs or irregularly sized triangular facets resulting from a paucity of last returns become apparent (Fig. 11).

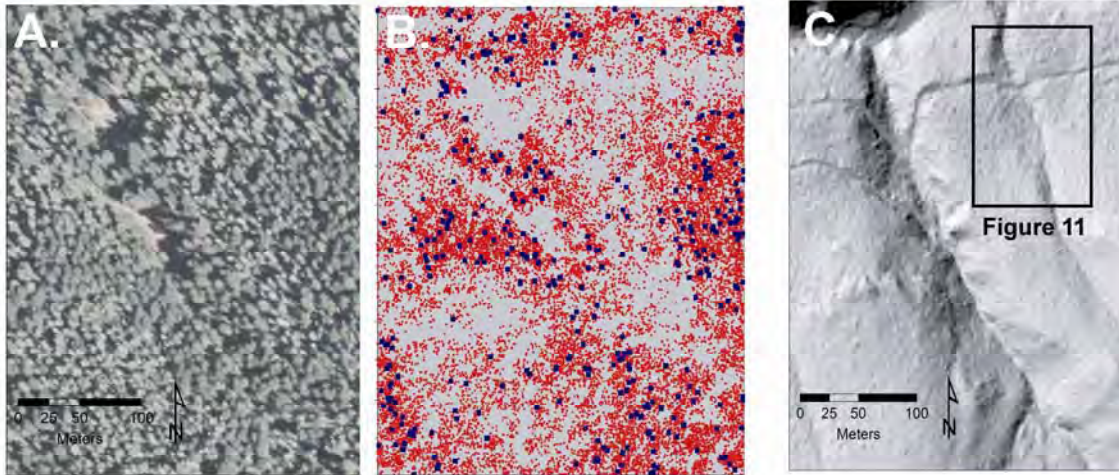


Figure 9. A. NAIP photograph of area near the Blue Jay mine, North Santiam mining district, Cascade Mountains, Oregon. B. LiDAR shot density of the area in A. Large blue squares represent 4th returns; small red squares represent 3rd returns. C. Hillshade of LiDAR DEMs of the Blue Jay mine area.

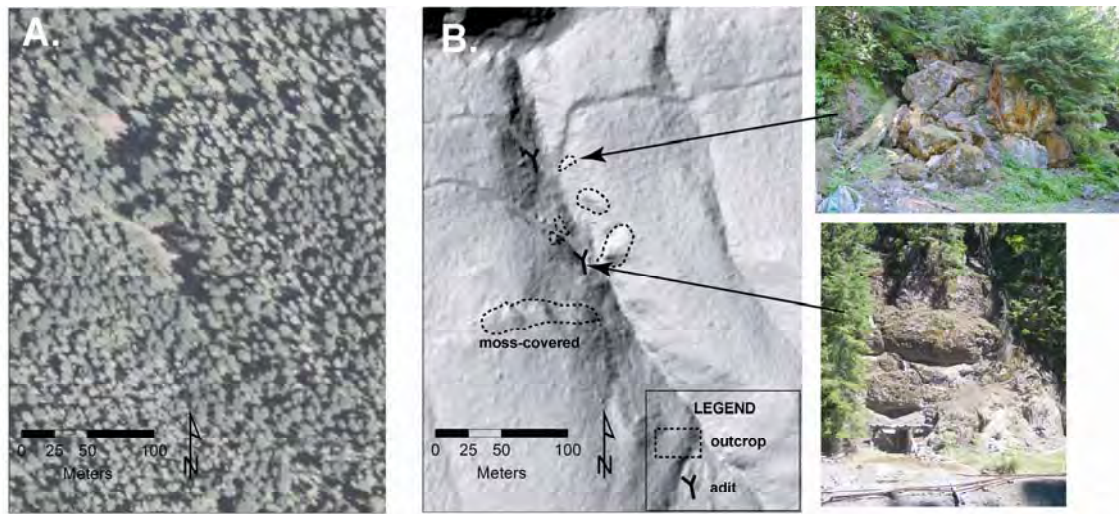


Figure 10. A. NAIP photograph of area near the Blue Jay mine, North Santiam mining district, Cascade Mountains, Oregon. B. Hillshade of LiDAR DEMs of the Blue Jay mine area Hillshade of LiDAR-derived DEMs showing location of outcrops and adits in the area.

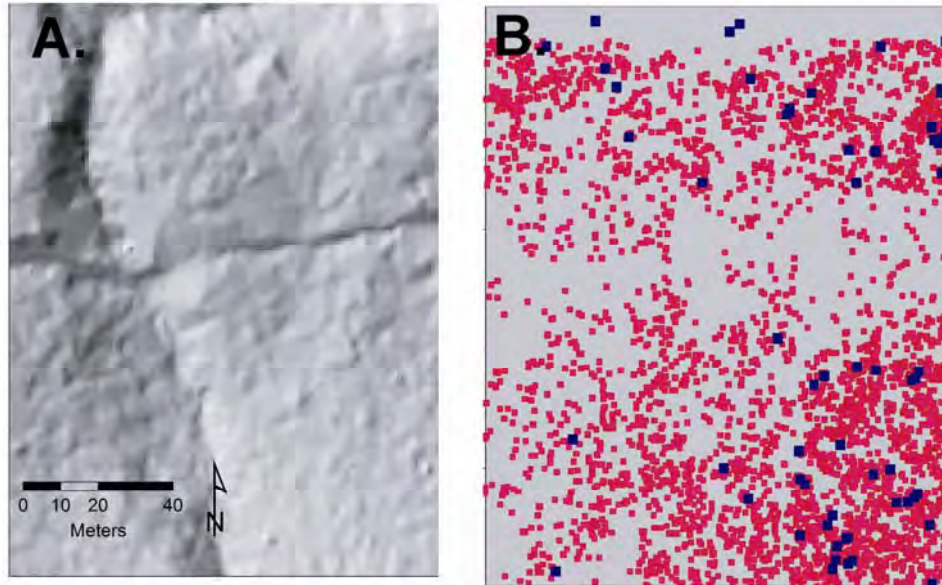


Figure 11. A. Detailed of hillshade of LiDAR-derived DEMs showing pits and triangular facets (“tinning”) as a result of sparse laser returns. B. Laser spot return density for area of A.

DISCUSSION

The examples shown here illustrate the importance high quality data acquisition and post-processing. To this end, vigorous QA/QC procedures must be following after LiDAR is flown and the data processed as results from the survey of the Frisco district shows. LiDAR data from heavily vegetated or forested terrain should be ground-truthed with high resolution GPS measurements and very crude DEMs can be expected where last return data are sparse (Fig. 11).

Once high-quality LiDAR data are obtained, standard geographic information (GIS) software can reveal many interesting geologic features. However, new software capable of enhancing geologic interpretations is continually appearing in this dynamic field. The MICRODEM program applied to the Thayne Canyon area (Fig. 5C) is but one example; other software packages are summarized on websites such as OpenTopography.org.

Geologic considerations

The results presented here were part of more extensive field investigations carried out by the authors and others at the University of Utah in Utah and Oregon. In many cases, the hydrothermal alteration features associated with mineralized areas were not visible with the LiDAR-derived DEMs. For instance, the accreted greenstone-volcanic terrain of the Blue Mountains of northeastern Oregon contains numerous historic vein gold deposits (Allen, 1951) and linear features were clearly visible in the DEMs, but none could be definitively related to observed mineralized structures on the ground. Similar difficulties were encountered in the western and southern portions of the Alta district where complex thrust and normal faulting are both pervasive.

However, as the three case studies presented above illustrate, LiDAR technology can be useful in areas where the geology is favorable. The technique appears most helpful where recessive linear features (e.g., fault in Thaynes Formation) (Fig. 5B) or resistant features in an otherwise uniform geologic landscape (e.g., jasperoids in massive limestone) (Fig. 7A) are present.

Outcrop identification is another area where LiDAR can play an important role in mineral exploration. The radius of visibility on the ground in places such as the Cascades of Oregon is sometimes no more than a few meters, and knowing the existence of outcrops, even when covered by moss (e.g., Fig. 10B) can be useful to the explorationist.

Piggy-backing with other geophysical techniques

It is envisioned that LiDAR could eventually become a complementary technique to more traditional airborne geophysical methods. A large expense of any airborne

geophysical survey is operation of the airborne platform (be it fixed wing or helicopter). Thus the current expense of airborne LiDAR surveys (estimated to be \$200-\$500/km²) could be pared down considerably were it mounted in the same aircraft as other geophysical instruments. Unfortunately, considerable differences exist in the standard routines for collecting both forms of data, principally in the flight heights of the airborne platforms. Airborne geophysical surveys are typically conducted at relatively low elevations (100s of m) while airborne LiDAR surveys are acquired at much higher elevations (1000s of m). However, LiDAR has the advantage that data can be collected at any distance; terrestrial surveys are done at ranges as close as a 1-2 m. Since the horizontal spacing of the LiDAR data decreases with distance to the target, low flying aircraft data could conceivably collect closely spaced (10s cm) data in conjunction with traditional geophysical instrumentation.

CONCLUSIONS

The digital revolution in the imaging surface geology has been brought about by the confluence of exponentially increasing computer power (as expressed by “Moore’s Law”) (Moore, 1965) and the technological advances of remote sensing instruments (Fig. 1). Exploration geologists, like all scientists, should become familiar with these new, rapidly advancing technologies and stand ready to incorporate them into their craft.

In order for the world to provide the raw materials for expanding economies, new mineral deposits must be located (1) at greater depths in mature mining districts or (2) in areas that are prospective but have not received as much attention as the traditional mining provinces of the western U.S. Examples of this latter category include the Precambrian shield of the upper Midwest (for instance the nickel deposit brought recently

into production in the Upper Peninsula of Michigan) and the majority of Alaska that remains open to mineral entry. Both of these areas are characterized by extensive boreal forest cover masking much of the geologic outcrops that can point the way toward potential ore deposits. Therein lies the promise of developing protocols for integrating airborne LiDAR into standard mineral exploration strategies.

Finally, it is important to emphasize the symbiotic possibilities between applying LiDAR to mineral exploration and the larger issue of LiDAR as a component of general U.S. infrastructure. To date, most airborne LiDAR surveys have been underwritten as components of academic research projects, state and municipal governments that use the data for urban planning, transportation, and flood plain mapping purposes, or land management agencies such as the U.S. Forest Service for specialized projects such as timber sales. Demonstrating the utility of LiDAR as a tool for mineral exploration could broaden overall public support for greater acquisition of these data which could then be used by both private and public entities. The so-called “Elevation for the Nation” initiative (National Research Council, 2007) is one such far-reaching possibility.

ACKNOWLEDGMENTS

Research supported by the U.S. Geological Survey (USGS), Department of the Interior, under USGS award number G11AP20050. The views and conclusions contained in this document are those of the authors and should not be interpreted as necessarily representing the official policies, either expressed or implied, of the U.S. Government. Additional help in the field was provided by Ryan Hamilton and Kimberlee

Pulsipher. Aid in understanding LiDAR processing was provided by Mike Boeder, Watershed Sciences, Inc.

REFERENCES

- Allen, R. M., Structural control of some gold-base metal veins in eastern Grant County, Oregon. *Economic Geology*, v. 46, p. 398-403.
- Baker, A.A., Calkins, F.C., Crittenden, M.D., JR., and Bromfield, C.S., 1966, Geologic Map of the Brighton Quadrangle, Utah: U. S. Geological Survey Quadrangle Map GQ-534.
- Bellian, J. A., Kerans, C., and Jennette, D. C., 2005, Digital outcrop models' applications for terrestrial scanning LiDAR technology in stratigraphic modeling. *Journal of Sedimentary Geology*, v. 75, p. 166-176.
- Boutwell, J.M., 1912, Geology and ore deposits of the Park City district, Utah, U. S. Geological Survey Professional Paper 77, p. 218-225
- Bromfield, C.S., 1989, Gold deposits in the Park City mining district, Utah, U. S. Geological Survey Bulletin, 1857-C, pp. C14-C26.
- Butler, B. S., 1913, Geology and ore deposits of the San Francisco and adjacent districts, Utah, *U. S. Geological Survey Professional Paper 80*, 212 p.
- Butler, B. S., 1914, Geology and ore deposits of the San Francisco and adjacent districts, Utah, *Economic Geology*, v. 9, p. 412-434.
- Calkins, F. C., and Butler, B. S., 1943, Geology and ore deposits of the Cottonwood-American Fork area, Utah. *U. S. Geological Survey Professional Paper 201*, 152 p.
- Callaghan, E. and Buddington, A. F., 1938, Metalliferous mineral deposits of the Cascade Range, Oregon. *U. S. Geological Survey Bulletin 893*, 141 p..

- Haaugerud, R. A., Harding, D. J., Johnson, S. Y., Harless, J. L., Weaver, C. S., and Sherrod, B. L., 2003, High resolution Lidar topography of Puget Sound Lowland, Washington – A bonanza for earth science, *GSA Today*, v. 13, no. 6, p. 4-10.
- Hedenquist, J. W., A. R. Aribas, and E. Gonzalez-Urien, 2000, Exploration for epithermal gold deposits, in *Gold in 2000*, S. G. Hageman and P. E. Brown, eds., *Reviews in Economic Geology*, v. 13, p. 245-277.
- Hintze, L. F., 1984, Geologic map of the Frisco Peak Quadrangle, Millard and Beaver Counties, Utah, U. S. Geological Survey Misc. Investigations Map I-1573.
- John, D.A., 1998, Geologic setting and characteristics of mineral deposits in the central Wasatch Mountains, Utah, *Geology and ore deposits of the Oquirrh and central Wasatch Mountains, Utah: Society of Economic Geologists Field Guidebook*.
- Jones, R. R., Kokkalas, S., McCaffrey, K. J. W., 2009, Quantitative analysis and visualization of nonplanar fault surfaces using terrestrial laser scanning (LIDAR)—The Arkitsa fault, central Greece, as a case study: *Geosphere*, v. 5, p. 465-482.
- Lovering, T. S., 1972, Jasperoid in the United States – Its characteristics, origin, and economic significance: *U. S. Geological Survey Professional Paper 710*, 164 p.
- Meier, C., 2005, Quality assurance review of LiDAR data for the Wah-Wah Valley, Beaver County, Utah. National Resource Conservation Service, Cedar City, Utah.
- Moore, G. E., 1965, Cramming more components onto integrated circuits. *Electronics*, v. 38
- National Research Council, 2007, *Elevation data for floodplain mapping*, National Academies Press, 151 p. Series no. 29, p. 11-33.
- Pavlis, T. L., and Bruhn, R. L., 2011, Application of LIDAR to resolving bedrock structure in areas of poor exposure: and example from the STEEP study area, southern Alaska, *Geological Society of America Bulletin*, v. 123, p. 206-217.
- Pringle, J.K., Westerman, A.R., Clark, J.D., Drinkwater, N.J. and Gardiner, A.R., 2004. 3D high-resolution digital models of outcrop analogue study sites to constrain

- reservoir model uncertainty: an example from Alport Castles, Derbyshire, UK.
Petroleum Geoscience, 10(4), pp. 343-352,
- Schenk, T., 1999, Digital photogrammetry. TerraScience, Laurelville, OH, 428 p.
- Schulz, W. H., 2005, Landslide susceptibility estimated from mapping using light detection and ranging (LiDAR) imagery and historical landslide records, Seattle Washington. *U. S. Geological Survey Open File Report 2005-1405*, 13 p.
- Silver, E., MacKnight, R., Male, E., Pickles, W., Cocks, P., and Wailbel, A., 2011, LiDAR and hyperspectral analysis of mineral alteration and faulting on the west side of the Humboldt Range, Nevada, *Geosphere*, v. 7, p. 1357-1368.
- Smith, L. C., 2002, Emerging applications of interferometric synthetic aperture radar (InSAR) in geomorphology and hydrology, *Annals of the Association of American Geographers*, v. 92, p. 385-398.
- Tilton, J.E., Eggert, R.G. and Landsberg, H.H., eds., 1988, World mineral exploration: Trends and economic issues: Washington, D.C., Resources for the Future, Inc., p. 343-349.